Efficient Metal-Free Catalytic Reaction Pathway for Selective Oxidation of Substituted Phenols

Yangming Lin,[†,‡] Bo Li,[†] Zhenbao Feng,[†] Yoong Ahm Kim,[§] Morinobu Endo,[∥] and Dang Sheng Su[*,†,⊥]

[†]Shenyang National Laboratory for Materials Science, Institute of Metal Research, Chinese Academy of Sciences, Shenyang, 110016 People's Republic of China

[‡]School of Chemistry and Materials Science, University of Science and Technology of China, Hefei, 230001 People's Republic of China

[§]School of Polymer Science and Engineering, Chonnam National University, 77 Yongbong-ro, Buk-gu Kwangju, 500-757 Republic of Korea

[∥]Carbon Institute of Science and Technology, Shinshu University, 4-17-1 Wakasato, Nagano, 380-8553 Japan

[⊥]Department of Inorganic Chemistry, Fritz Haber Institute of the Max Planck Society, Faradayweg 4-6, Berlin, 14195 Germany

S *Supporting Information*

ABSTRACT: Selective oxidation of substituted phenols to *p*-benzoquinones is known to be inefficient because of the competing C−O coupling reaction caused by phenoxy radicals. The poor stability of conventional metal-based catalysts represents another bottleneck for industrial application. Here, we describe a metal-free reaction pathway in which onion-like carbon (OLC) as a low-cost catalyst exhibits excellent catalytic activity and stability in the selective oxidation of mono-, di- and trisubstituted phenols to their corresponding *p*-benzoquinones, even better than the reported metal-based catalysts (e.g., yield, stability) and industrial catalysts for particular substrates.

Together with XPS, Raman, DFT calculations, and a series of comparative experiments, we demonstrate that the zigzag configuration as a type of carbon defects may play a crucial role in these reactions by stabilizing the intermediate phenoxy radicals.

KEYWORDS: onion-like carbon, molecular model catalysts, phenol, selective oxidation, metal-free
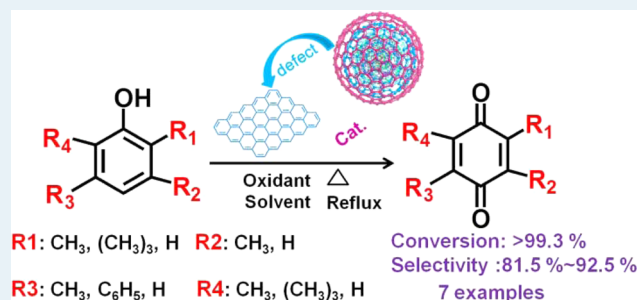
Natural products with a benzoquinone structure typically play an important role in biomedicine and the synthesis of fine chemical compounds.[1,2] For example, 2,6-di-*tert*-butyl-1,4-benzoquinone (DTBQ) is a highly active antioxidant with antiaging properties.[3] 2-Methyl-1,4-naphthoquinone (MNQ, vitamin K3) is a kind of popular coagulant.[4,5] 2,3,5-Timethyl-1,4-benzoquinone (TMBQ) is an important key intermediate of vitamin E. Traditionally, selective oxidation preparation of *p*-benzoquinones from the substituted phenols is known to be inefficient because of the rather favorable C−O coupling reaction, as facilitated by phenoxy radicals.[6,7] Current studies have focused on various metal-based catalysts, such as Co(II)−Schiff base complexes,[8] supported heteropolycompounds,[9,10] molecular sieves,[11−14] heteropoly acids,[15] and noble metal catalysts.[16] For the reaction pathways, alternative routes in the presence of H_2O_2 or O_2 have been developed to improve the yields of desired products in a homogeneous catalytic environment. The yields of target *p*-benzoquinones by these approaches could reach to ~55−93%.[4,17−29] Despite this, the drawbacks of these methods involve low selectivity of the desired *p*-benzoquinones, the overproduction of byproducts (e.g. dimeric or polymeric C−O coupling products),
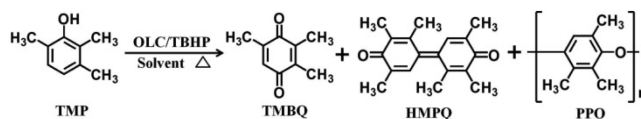
cumbersome preparation processes, inactivation and structure shrinkage of the catalysts, high toxicity of the catalysts, and required strongly acidic/highly corrosive conditions. Development a new catalytic system with high efficiency and a smaller environmental footprint for the production of various *p*-benzoquinones is therefore demanded.

Metal-free nanocarbon materials have been shown to be alternative candidates to conventional metal-based catalysts for some important reactions.[30−34] Onion-like carbon (OLC) obtained by a high-temperature thermal treatment (1500−1800 °C; see Figure S8 of the Supporting Information) of nanodiamond in a graphite furnace exhibits a quasi-spherical morphology consisting of multiple closed concentric fullerene-like shells and possesses some unique chemical and physical properties.[35,36] OLC have been widely investigated for gas-phase catalytic reactions, magnetic materials, electrode materials, and supercapacitors.[37−40]

Table 1. Catalytic Oxidation of 2,3,6-Trimethylphenol (TMP) over Various Samples under Different Conditions[a]

entry	catalyst	S_{BET} (m² g⁻¹)	T (°C)	conv. (%)	sel. (%) TMBQ	sel. (%) HMPQ	sel. (%) PPO	yield (%) TMBQ
1[b]			80	16.5	13.9	3.1	81.1	2.3
2	OLC-1	463	80	99.8	82.5	15.7	trace	82.3
3	OLC-2	476	80	91.6	72.1	25.2	trace	66.1
4	OLC-3	459	80	88.6	72.3	25.8	trace	64.1
5	OLC-4	430	80	60.1	45.5	52.2	trace	27.4
6	AC	1178	80	52.4	30.4	66.7	trace	15.9
7	graphite		80	30.3	24.9	73.2	trace	7.5
8	UDD	305	80	65.5	13.4	84.3	trace	8.8
9	HHT	35	80	40.1	32.3	61.6	trace	13.0
10[c]	graphene	520	80	81.4	58.9	39.2	trace	47.9
11[d]	OLC-1	463	80	44.8	13.5	81.7	trace	6.0
12[e]	OLC-1	463	80	97.3	42.5	55.4	trace	41.4
13[f]	Ti-HMS		60	97	87			84.3
14[g]	Ti-HMS		60	3	66.7			2
15[h]	Ti−Si	1288	80	100	100			100
16[i]	Ti−Si	1288	80	90	99			89
17[j]	OLC-1	463	80	99.1	76.7	19.7	trace	76.0
18[k]	40% H₂SO₄		60−70	>99	>85			>85
19[l]	CuCl₂ MgCl₂		80	>99	>90			>90

[a]Reaction conditions: 8 mg of catalyst, 0.1 mmol of substrate, 0.36 mmol of *tert*-butyl hydroperoxide (TBHP), 5 mL of TFT solvent, t = 12 h. [b]Conducted in the absence of catalyst. [c]Obtained from ref 42, the S_{BET} was recorded on the Micromeritics ASAP2020 analyzer. [d]The reaction conditions are the same as in footnote *a*, except the oxidant is 30% H₂O₂. [e]The reaction conditions are the same as in footnote *a*, except the oxidant is cumyl hydroperoxide. [f]Reference 16, 200 mg of catalyst, t = 240 min, $n(H_2O_2)/n(phenol)$ = 1, MeOH as solvent. [g]The reaction conditions are the same as in footnote *f*, except the oxidant is TBHP. [h]Reference 11, 20 mg of catalyst, t = 40 min, 0.1 mmol of substrate, 0.44 mmol of H₂O₂, 1 mL of CH₃CN solvent. [i]The seventh cycle test of catalyst under the footnote *h* conditions. [j]7 g of catalyst, 12 g of substrate, 3.6 equiv of TBHP, 200 mL of TFT solvent, t = 12 h. [k]MnO₂ as oxidant. [l]O₂ as oxidant. Desired product: 2,3,5-timethyl-1,4-benzoquinone (TMBQ). Byproducts: 2,2,3,3,5,5-hexamethyl-4,4-diphenoquinone (HMPQ), polyphenylene oxide (PPO).

In the present study, we demonstrate the excellent catalytic acitivity of OLC for selective oxidation of representative substituted phenols (seven examples) to their corresponding *p*-benzoquinones. To the best of our knowledge, it is the first time that the substitute phenol has been catalyzed by metal-free nanocarbons with decent activity. From XPS, Raman, and other comparative experiments, we show that the zigzag configuration rather than the oxygen species is responsible for the enhanced activities for these catalytic reactions.

Figure S9A−D shows the structures of various OLC samples consisting of multilayer sp² fullerene-like shells. The identified interlayer spacing of ∼0.340 nm in the shell of OLC is assigned to the (002) of turbostratic carbon graphite.[41] The particle sizes of all OLC samples are ∼5−8 nm, and some lattice disorder can be observed on the OLC samples (Figure S9, marked by red arrows). Regarding the N₂ physisorption results, there is only a small difference in the surface area of the OLC samples (Figure S10 and Table 1).

Table 1 displays the catalytic performances of various carbon materials for the selective oxidation of 2,3,6-trimethylphenol (TMP) to 2,3,5-trimethyl-1,4-benzoquinone (TMBQ) under different conditions. Without catalysts, only 2.3% of TMBQ yield was obtained (Table1, entry 1) and the main byproduct was polyphenylene oxide (PPO). The TMP conversion and the selectivity of the desired TMBQ over the four kinds of OLC samples were at reasonably high levels (Table1, entries 2−5). Among the four OLC samples treated at different temperatures,

OLC-1 (treated at 1500 °C) exhibited the best catalytic performance, with a TMBQ yield of 82.3% under the optimized reaction conditions (entry 2). In contrast, some other carbon materials, such as activated carbon (AC, entry 6), graphite (entry 7), UDD (entry 8), HHT (a commercial high-temperature-treated nanocarbon fiber with well graphitized structure; entry 9 Figure S11);), and graphene (G250, entry 10),[42] showed a lower yield of TMBQ (∼7.5−47.9%) under the same reaction conditions. In addition, the dependences of catalytic performance on time, the amount of TBHP, temperature, the solvent type, and the oxidant were studied in detail, and the results are listed in Figure S12 and Table 1, entries 11−12. Long reaction times; elevated reaction temperatures; and increased amounts of TBHP and other oxidants, including cumyl hydroperoxide and hydrogen peroxide, were not favorable for improving the selectivity of TMBQ over OLC-1.

As shown in Figure 1A, the conversion of TMP over OLC-1 is 99.2% along with a TMBQ selectivity of 81.4% after seven successive runs, indicating that OLC-1 can be repeatedly used. This catalyst stability was further demonstrated by a low conversion experiment (the initial conversion of TMP was maintained at ∼20%, Figure 1B). Although the OLC-1 did not exhibit better catalytic activity than the reported Ti-HMS and Ti−Si catalysts using H₂O₂ as oxidant, it had a remarkable stability in the selective oxidation of TMP (Table 1, entries 11, 12, 15, 16). Interestingly, the activity of OLC-1 was far more
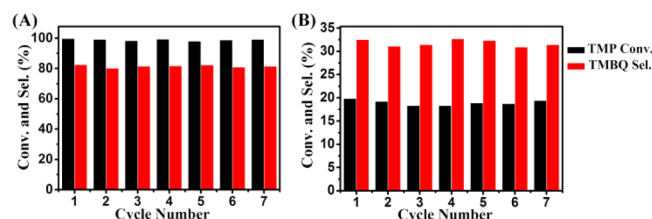
Figure 1. (A) Recycling test of OLC-1 for selective oxidation of TMP to TMBQ. Reaction conditions: 8 mg of catalyst, 0.1 mmol of substrate, 0.36 mmol of TBHP, 5 mL of TFT solvent, T = 80 °C, t = 12 h. (B) Recycling test of OLC-1 for selective oxidation of TMP to TMBQ. Reaction conditions: 8 mg of catalyst, 0.1 mmol of substrate, 0.36 mmol of TBHP, 5 mL of TFT solvent, T = 40 °C, t = 30 min.

than the Ti-HMS catalyst using TBHP as an oxidant (Table 1, entry 14). It should be noted that OLC-1 still displayed the good catalytic performance at preparative production scale (entry 17). Compared with the conventional homogeneous industrial catalysts (40% H_2SO_4 and $CuCl_2$ + $MgCl_2$), OLC-1 not only showed a competing catalytic performance but also represented a smaller environmental footprint for the production of TMBQ (Table 1, entries 18, 19).

Following the success of TMP oxidation, we applied OLC-1 to a series of phenols with mono-, di-, and other trisubstituted structures (Table 2). For all these derivatives, there was a reasonable conversion and selectivity output. For instance, TMBQ was produced efficiently from 2,3,5-trimethylphenol (2,3,5-TMP) and had a conversion of around 100% and selectivity of 87.5% at 100 °C after 12 hours (Table 2, entry 1). The selective oxidation for di-substituted phenols, including 2,6-dimethylphenol (DMP), 2,6-dimethylphenol (2,5-DMP) and 2-methyl-1-naphthol (MNL) resulted in ∼80.9−85.7% yield of the corresponding *p*-benzoquinones under the optimized reaction conditions (Table 2, entries 2, 4, 6 and Figure S14). Compared with the reported metal-based catalysts and the industrial homogeneous catalyst (CrO_3/CH_3COOH/H_2SO_4),[9,16] OLC-1 exhibited an excellent catalytic performance in the selective oxidation of DMP, 2,6-di-*tert*-butyl phenol (DTBP) and MNL under similar reaction conditions (Table 2, entries 2, 3, 6). Moreover, a good catalytic performance for the oxidation of mono-substituted phenol, 2-methylphenol (MP), can be achieved as expected (Table 2, entry 5). Thus, a cost-effective metal-free catalytic system to realize the selective oxidation of phenols has been achieved.

To study the origin of the catalytic performance of OLC, XPS was employed to investigate the surface composition of the catalysts. Figure S15A illustrates that with an increase in the preparation temperature, the full width at half-maximum (fwhm) value of C 1s spectra decreases from 1.21 eV for OLC-1 to 1.11 eV for OLC-4. This sugguests that OLC-4 has a more ordered graphitic structure. As shown in Figure S15B, all the catalysts have similar oxygen concentrations (0.53−0.64 at. %). This is also confirmed by elemental analysis (0.33−0.38 wt %, Table S1). The oxygen peaks located at 530.8 and 533 eV were assigned to trace C=O and C−O (ether group) or C−OH groups, respectively.[35] As reported earlier, oxygen species, such as a carbonyl group, have been proven to be the active sites in alkane oxidative dehydrogenation and nitrobenzene reduction reactions.[43,44] In the present work, OLC-4 with C=O group did not exhibit the best catalytic performacne. This signifies that C=O is perhaps not critical to the phenol oxidation reaction. In addition, the three other catalysts with

Table 2. Catalytic Oxidation of Various Substituted Phenols over OLC-1 Catalyst[a]

Entry	Substrate	Product	Conv. (%)	Sel. (%)	Yield (%)
1[b]	(2, 3, 5-TMP)	(TMBQ)	99.8	87.5	87.3
2[c]	(DMP)	(DMBQ)	99.3 100[f]	81.5 59[f]	80.9 59[f]
3[d]	(DTBP)	(DTBQ)	99.7 87[g] 5[h]	92.5 81.6[g] 80[h]	92.3 71[g] 4[h]
4	(2, 5-DMP)	(2, 5-DMBQ)	99.8	85.9	85.7
5	(MP)	(MBQ)	99.5	82.1	81.7
6[e]	(MNL)	(MNQ)	99.6 >99[i]	84.2 ∼50[i]	83.8 ∼50[i]

[a]Reaction condition: 8 mg of OLC-1 catalyst, 0.1 mmol of substrate, 0.36 mmol of TBHP, 5 mL of TFT solvent, T = 80 °C, t = 4 h. [b]T = 100 °C, t = 14 h. [c]t = 5 h. [d]t = 8 h. [e]0.05 mmol of substrate, T = 70 °C, t = 12 h. [f]Reference 9, 1 mmol of substrate, 5 mLof acetone, 0.02 mmol of Cs3H1M11PV1 heterogeneous catalyst, 22 mmol H_2O_2, T = 20 °C, t = 7 h. [g]Reference 16, 200 mg of Ti-HMS catalyst, $n(H_2O_2)$/n(phenol) = 1, MeOH as solvent, T = 60 °C, t = 24 h. [h]The reaction conditions are the same as in footnote [f], except the oxidant is TBHP. [i]CrO_3/ CH_3COOH/H_2SO_4 catalyst, T = 60−90 °C

similar XPS O 1s spectral profiles (only C−O/C−OH group) showed different activities (Table 1, entries 2−4); hence, there is no simple correlation between the oxygen species and the observed catalytic performance. These results indicate that oxygen species might not be the active sites in the selective oxidation of the substituted phenols.

The Raman spectra of the OLC samples have three main features in the 1000−3000 cm^{-1} region (Figure S16A): D band (defect-induced mode, ∼1323 cm^{-1}), the G band (1578 cm^{-1}), and the 2D band (2652−2678 cm^{-1}). Compared with other OLC samples, the decreasing fwhm of the D band on OLC-4 represented a more ordered carbon network structure (Figure S16B). In contrast, OLC-1 had a more disordered carbon structure. The increased intensity, the asymmetric spectral profile, and the upshift (from 2652 to 2678 cm^{-1}) of the 2D band of the OLC samples reflected that the carbon structures consisting of stacked graphene layers were favorable to formation of an ordered carbon lattice under elevated temperature.[35,36,45] Moreover, Figure S17 illustrates that there is no obvious change between fresh OLC-1 and used OLC-1, suggesting the structural stability of OLC-1 catalyst. The I_D/I_G ratio was used to depict the number of defects, especially at graphene edges.[46] The linear relationship of the activity with the I_D/I_G ratio in Figure 2 reveals that the ratio is proportional to the mass-normalized activity and the area-normalized activity
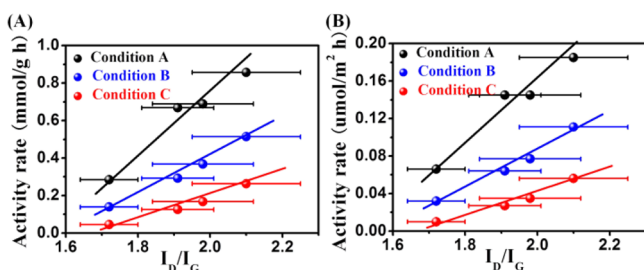
Figure 2. Dependences of mass-normalized activity (A) and area-normalized activity (B) on the I_D/I_G ratio under different reaction conditions in the selective oxidation of TMP to TMBQ. Condition A: 80 °C, 12 h. Condition B: 70 °C, 12 h. Condition C: 60 °C, 3 h.

under different reaction conditions, that is, the OLC-1 catalyst with the highest number of defects exhibits the best catalytic performance. The same linear relationship could be observed in the selective oxidation of DMP to DMBQ (Figure S18). In addition, when commercial HHT with a very low I_D/I_G ratio (∼0.35) was used in the oxidation reaction of TMP, a low yield (∼13%) was obtained (Table 1, entry 9). All the results showed that defects played a key role in these catalytic reactions.
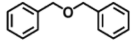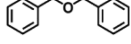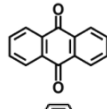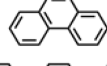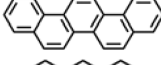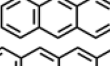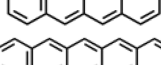
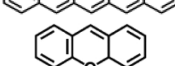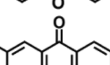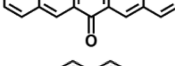Defects are rich in nanocarbons, and it has been reported that many reactions are catalyzed by the defects in carbon;[31,47] however, an effective method to identity the type of defect and to give an accurate description of the amounts of each type is lacking, even for the total number of defects per square (nano) meter. It is a challenge to identify the actual active sites because of the diversity of defects and technical limitations. Although first-principles calculation was used to study the influence of the doped Stone−Wales defect structure on ORR,[48] exploring the specific structure of active defect sites in a reaction process is still an arduous task. Here, we applied several small molecules as model catalysts to simulate the structures of carbon catalysts and to identify possible active sites.

As mentioned, the trace C═O and C−O group could be observed in OLC samples. When different loadings of benzyl ether and anthraquinone with the mimicked C═O and C−O structures were added into the reaction (Table 3, entries 2−4), it was found that the catalytic activities did not change as compared with the blank experiment. This again illustrates that the surface oxygen species is inconsequential to the catalytic reaction.

We also employed a few model catalysts with specific armchair and zigzag defect structures to identify the types of active sites. As shown in Table 3, two kinds of model catalysts with an armchair structure do not exhibit an enhanced catalytic performance (entries 5, 6). It is worth noting that with an increae in the zigzag unit (Table 3, entries 7−9 and Table S2), anthracene, naphthacene, and pentacene have an increasing yield in the selective oxidation of TMP (from 2.7% to 8.4%). A similar activity tendency for the model catalysts was observed in the selective oxidation of DMP to DMBQ (Figure S19). All the facts indicated that the zigzag configuration might have a positive effect on these reactions. In addition, there was no obvious synergistic effect between the zigzag and oxygen species (C═O, C−O), as well as for armchair structures because the yields of TMBQ were only 1.7%, 1.8%, and 2.5% on xanthenes, pentacenequinone, and coronene catalyst (entries 10−12), respectively.

As shown in Table S3, only 4.5% TBHP (about 0.0162 mmol) decomposed under the blank reaction conditions, which

Table 3. Catalytic Performance of TMP over Various Model Molecule Catalysts[a]

Entry	Model catalyst	Mimicked structure	Con. (%)	Sel. (%)	Yield (%)
1[b]	Blank	----	16.5	13.9	2.3
2		ether	18.5	14.2	2.6
3[c]		ether	18.8	14.1	2.7
4[c]		quinones	15.9	12.5	2.0
5		armchair	17.3	13.6	2.4
6		armchair	18.1	11.9	2.2
7		zigzag	18.2	14.8	2.7
8		zigzag	23.8	17.7	4.2
9		zigzag	37.3	22.5	8.4
10[c]		zigzag ether	15.1	11.1	1.7
11		zigzag quinones	25.1	7.1	1.8
12[c]		zigzag armchair	17.1	14.5	2.5

[a]Reaction conditions: 8 mg of model catalyst, 0.1 mmol of substrate, 0.36 mmol of TBHP, 5 mL of TFT solvent, T = 80 °C, 12 h. [b]Conducted in the absence of catalyst. [c]20 mg model catalysts. Desired product: 2,3,5-timethyl-1,4-benzoquinone (TMBQ).

is consistent with the conversion rate of TMP (16.5%), indicating the direct effect of TBHP on the TMP conversion. In contrast, the decomposition rate of TBHP over OLC-1 was 85.2%, suggesting that the fullerene-like shells had an excellent decomposition ability for TBHP. It has been reported that the selective oxidation of substituted phenols may involve a phenoxy radical coupling process.[50−52] The hydroxyl radical derived from the decomposition of TBHP would get close to the hydroxyl of the substituted phenol to abstract hydrogen (this is also the reason for a blank experiment with the TMP conversion of 16.5%),[33,53,54] and then the phenoxy radical was produced along with the release of water.[50−52,55] As mentioned above (Table 1, entry 1), the main product of the TMP oxidation was PPO (81.1% selectivity) in the absence of catalyst. This result was ascribed to the C−O coupling of phenoxy radicals. Thus, avoiding the C−O coupling must be a key step.

It has been suggested in the literature that the zigzag edge may be more reactive than the armchair edge due to its unique electronic structure and unpaired electrons.[56,57] It is therefore reasonable to expect that the phenoxy radical would be more stable for binding at the zigzag edge than the amchair edge.

To test this hypothesis, DFT calculations were performed to study the adsorption of the phenoxy radical at the model

catalysts, as shown in Table 3. In Figure 3, the adsorption of the phenoxy radical at the zigzag edge (five benzene rings) is
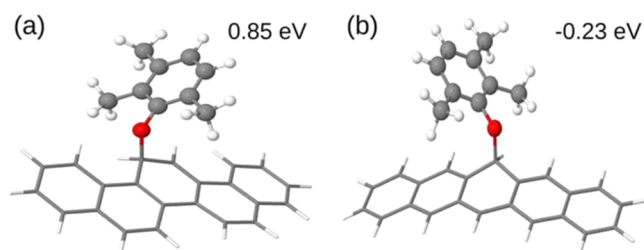

Figure 3. Adsorption energies and structures of phenoxy radical obtained from DFT calculations. (a) Armchair edge (model catalyst 6 in Table 3), (b) zigzag edge (model catalyst 9 in Table 3). The negative adsorption energy means the adsorption is exothermic. The structure optimization is carried out at the B3LYP/6-31G* level, and the energy is further refined at the B3LYP/6-311G* level of theory. All calculations are performed by using the Gaussian 09 code.[49] Color code: carbon is gray, hydrogen is white, and oxygen is red.

exothermic by 0.23 eV, and it becomes endothermic by 0.85 eV when the adsorption occurs at an armchair edge. The calculations clearly indicate that the zigzag edge plays an important role in stabilizing the phenoxy radical and, hence, restraining the coupling reaction of C−O on phenoxy radicals. Subsequently, it could be that a bound phenoxyl continues to react with the TBHP to afford the corresponding hydroquinone, which would then be readily oxidized by TBHP and finally achieve a high selectivity of the desired *p*-benzoquinone products. We believe that a clearer understanding of the mechanism is still required.

In summary, we have developed a metal-free heterogeneous catalytic reaction pathway for selective oxidation of substituted phenols to *p*-benzoquinones. Onion-like carbon as an efficient catalyst exhibited high conversion (>99.3%) and selectivity (~81.5−92.5%) toward substituted phenols at a mild reaction condition. It was found that the defects at a zigzag edge played an important role in these reactions. The catalytic performance may be attributed to the stabilization of intermediate phenoxy radicals at the zigzag configuration, as elucidated by the experimental results and theoretical studies. Our work provides a new opportunity for the development of metal-free catalysts and some valuable information for insight into the role of defects in carbon materials in liquid-phase catalytic reactions.

■ ASSOCIATED CONTENT

Ⓢ Supporting Information

The Supporting Information is available free of charge on the ACS Publications website at DOI: 10.1021/acscatal.5b01222.

> Materials, additional data and figures about the BET analysis, elemental analysis, Raman spectra, XPS spectra, and catalytic reaction conditions for various samples (PDF)

■ AUTHOR INFORMATION

Corresponding Author

*Phone: +86-24-83970029. Fax: +86-24-83970019. E-mail: dssu@imr.ac.cn.

Notes

The authors declare no competing financial interests.

■ REFERENCES

(1) (a) Saladino, R.; Neri, V.; Mincione, E.; Filippone, P. *Tetrahedron* **2002**, *58*, 8493−8500. (b) Fishwick, C.W. G.; Jones, D. W. *The Quinonoid Compounds*; Patai, S., Ed.; Wiley: Chichester, 1988; Vol. *1*, pp 403−453. (c) Finley, K. T. *The Quinonoid Compounds*; Patai, S., Ed.; Wiley: Chichester, 1988; Vol. *1*; pp 537 − 717. (d) Mariarty, R. M.; Prakash, O. M. *Organic Reactions*; Wiley, Hoboken, 2004, 327 − 415.

(2) Takaki, K.; Shimasaki, Y.; Shishido, T.; Takehira, K. *Bull. Chem. Soc. Jpn.* **2002**, *75*, 311−317.

(3) Mohapatra, S. K.; Hussain, F.; Selvam, P. *Catal. Commun.* **2003**, *4*, 57−62.

(4) Bohle, A.; Schubert, A.; Sun, Y.; Thiel, W. R. *Adv. Synth. Catal.* **2006**, *348*, 1011−1015.

(5) Sheldon, R. A.; Dakka, J. *Catal. Today* **1994**, *19*, 215−245.

(6) Boldron, C.; Aromi, G.; Challa, G.; Gamez, P.; Reedijk, J. *Chem. Commun.* **2005**, 5808−5810.

(7) Murahashi, S. I.; Naota, T.; Miyaguchi, N.; Noda, S. *J. Am. Chem. Soc.* **1996**, *118*, 2509−2510.

(8) Gupta, K. C.; Sutar, A. K. *Coord. Chem. Rev.* **2008**, *252*, 1420−1450.

(9) Villabrille, P.; Romanelli, G.; Vázquez, P.; Cáceres, C. *Appl. Catal., A* **2004**, *270*, 101−111.

(10) Villabrille, P.; Romanelli, G.; Vázquez, P.; Cáceres, C. *Appl. Catal., A* **2008**, *334*, 374−380.

(11) Ivanchikova, I. D.; Kovalev, M. K.; Mel'gunov, M. S.; Shmakov, A. N.; Kholdeeva, O. A. *Catal. Sci. Technol.* **2014**, *4*, 200−207.

(12) Kholdeeva, O. A.; Zalomaeva, O. V.; Shmakov, A. N.; Melgunov, M. S.; Sorokin, A. B. *J. Catal.* **2005**, *236*, 62−68.

(13) Tanev, P. T.; Chibwe, M.; Pinnavaia, T. J. *Nature* **1994**, *368*, 321−323.

(14) Kholdeeva, O. A. *Catal. Sci. Technol.* **2014**, *4*, 1869−1889.

(15) Ivanchikova, I. D.; Maksimchuk, N. V.; Maksimovskaya, R. I.; Maksimov, G. M.; Kholdeeva, O. A. *ACS Catal.* **2014**, *4*, 2706−2713.

(16) Cheneviere, Y.; Caps, V.; Tuel, A. *Appl. Catal., A* **2010**, *387*, 129−134.

(17) Möller, K.; Wienhöfer, G.; Schröder, K.; Join, B.; Junge, K.; Beller, M. *Chem. - Eur. J.* **2010**, *16*, 10300−10303.

(18) Wienhöfer, G.; Schröder, K.; Möller, K.; Junge, K.; Beller, M. *Adv. Synth. Catal.* **2010**, *352*, 1615−1620.

(19) Hay, A. S. U.S. Patent 3,306,874 [P], 1967-2-28.

(20) Rutledge, T. U.S. Patent 3,784,575[P], 1974-1-8.

(21) Costantini, M.; Jouffret, M. U.S. Patent 4,208,339[P], 1980-6-17.

(22) Michelet, D.; Razoutz, M. U.S. Patent 3,927,045[P], 1975-12-16.

(23) Braxton, J. H. G.; Closson, R. D. U.S. Patent 3,213,114[P], 1965-10-19.

(24) Reilly, E. L. U.S. Patent 4,257,968[P], 1981-3-24.

(25) Dietl, H. K.; Young, H. S. U.S. Patent 4,360,469[P], 1982-11-23.

(26) Pommer, H.; Schuster, L. U.S. Patent 3,658,852[P], 1972-4-25.

(27) Rappoport, Z.; Yamamura, S. *Oxidation of Phenols*; Wiley: West Sussex, U.K, 2003; pp 1153−1346. DOI: 10.1002/0470857277.ch17.

(28) Molander, G. A.; Knochel, P. *Comprehensive Organic Synthesis*, 2nd ed.; Elsevier: Oxford, 2014, Vol. *3*; pp 56−740.

(29) Allen, S. E.; Walvoord, R. R.; Padilla-Salinas, R.; Kozlowski, M. C. *Chem. Rev.* **2013**, *113*, 6234−6458.

(30) Qi, W.; Su, D. *ACS Catal.* **2014**, *4*, 3212−3218.

(31) Su, D. S.; Perathoner, S.; Centi, G. *Chem. Rev.* **2013**, *113*, 5782−5816.

(32) Lin, Y.; Su, D. *ACS Nano* **2014**, *8*, 7823−7833.

(33) Li, W.; Gao, Y.; Chen, W.; Tang, P.; Li, W.; Shi, Z.; Su, D. S.; Wang, J.; Ma, D. *ACS Catal.* **2014**, *4*, 1261−1266.

(34) Cao, Y.; Yu, H.; Peng, F.; Wang, H. *ACS Catal.* **2014**, *4*, 1617−1625.

(35) Lin, Y.; Pan, X.; Qi, W.; Zhang, B.; Su, D. S. *J. Mater. Chem. A* **2014**, *2*, 12475−12483.

(36) Holec, D.; Hartmann, M. A.; Fischer, F. D.; Rammerstorfer, F. G.; Mayrhofer, P. H.; Paris, O. *Phys. Rev. B: Condens. Matter Mater. Phys.* **2010**, *81*, 235403.

(37) Keller, N.; Maksimova, N. I.; Roddatis, V. V.; Schur, M.; Mestl, G.; Butenko, Y. V.; Kuznetsov, V. L.; Schlögl, R. *Angew. Chem., Int. Ed.* **2002**, *41*, 1885−1888.

(38) Shenderova, O.; Grishko, V.; Cunningham, G.; Moseenkov, S.; McGuire, G.; Kuznetsov, V. *Diamond Relat. Mater.* **2008**, *17*, 462−466.

(39) Li, S.; Feng, G.; Fulvio, P. F.; Hillesheim, P. C.; Liao, C.; Dai, S.; Cummings, P. T. *J. Phys. Chem. Lett.* **2012**, *3*, 2465−2469.

(40) Pech, D.; Brunet, M.; Durou, H.; Huang, P.; Mochalin, V.; Gogotsi, Y.; Taberna, P. L.; Simon, P. *Nat. Nanotechnol.* **2010**, *5*, 651−654.

(41) Lin, Y.; Wu, S.; Shi, W.; Zhang, B.; Wang, J.; Kim, Y. A.; Endo, M.; Su, D. S. *Chem. Commun.* **2015**, *51*, 13086−13089.

(42) Chen, C. M.; Zhang, Q.; Zhao, X. C.; Zhang, B.; Kong, Q. Q.; Yang, M. G.; Yang, Q. H.; Wang, M. Z.; Yang, Y. G.; Schlogl, R.; Su, D. S. *J. Mater. Chem.* **2012**, *22*, 14076−14084.

(43) Wu, S.; Wen, G.; Liu, X.; Zhong, B.; Su, D. S. *ChemCatChem* **2014**, *6*, 1558−1561.

(44) Zhang, J.; Liu, X.; Blume, R.; Zhang, A. H.; Schlögl, R.; Su, D. S. *Science* **2008**, *322*, 73.

(45) Bogdanov, K.; Fedorov, A.; Osipov, V.; Enoki, T.; Takai, K.; Hayashi, T.; Ermakov, V.; Moshkalev, S.; Baranov, A. *Carbon* **2014**, *73*, 78−86.

(46) Wang, Y.; Alsmeyer, D. C.; McCreery, R. L. *Chem. Mater.* **1990**, *2*, 557−563.

(47) Song, S.; Yang, H.; Rao, R.; Liu, H.; Zhang, A. *Catal. Commun.* **2010**, *11*, 783−787.

(48) Chai, G. L.; Hou, Z.; Shu, D. J.; Ikeda, T.; Terakura, K. *J. Am. Chem. Soc.* **2014**, *136*, 13629−13640.

(49) Frisch, M. J.; Trucks, G. W.; Schlegel, H. B.; Scuseria, G. E.; Robb, M. A.; Cheeseman, J. R.; Scalmani, G.; Barone, V.; Mennucci, B.; Petersson, G. A.; Nakatsuji, H.; Caricato, M.; Li, X.; Hratchian, H. P.; Izmaylov, A. F.; Bloino, J.; Zheng, G.; Sonnenberg, J. L.; Hada, M.; Ehara, M.; Toyota, K.; Fukuda, R.; Hasegawa, J.; Ishida, M.; Nakajima, T.; Honda, Y.; Kitao, O.; Nakai, H.; Vreven, T.; Montgomery, J. A., Jr.; Peralta, J. E.; Ogliaro, F.; Bearpark, M. J.; Heyd, J.; Brothers, E. N.; Kudin, K. N.; Staroverov, V. N.; Kobayashi, R.; Normand, J.; Raghavachari, K.; Rendell, A. P.; Burant, J. C.; Iyengar, S. S.; Tomasi, J.; Cossi, M.; Rega, N.; Millam, N. J.; Klene, M.; Knox, J. E.; Cross, J. B.; Bakken, V.; Adamo, C.; Jaramillo, J.; Gomperts, R.; Stratmann, R. E.; Yazyev, O.; Austin, A. J.; Cammi, R.; Pomelli, C.; Ochterski, J. W.; Martin, R. L.; Morokuma, K.; Zakrzewski, V. G.; Voth, G. A.; Salvador, P.; Dannenberg, J. J.; Dapprich, S.; Daniels, A. D.; Farkas, Ö.; Foresman, J. B.; Ortiz, J. V.; Cioslowski, J.; Fox, D. J. *Gaussian 09*; Gaussian, Inc.: Wallingford, CT, USA, 2009.

(50) Esguerra, K. V. N; Fall, Y.; Petitjean, L.; Lumb, J. P. *J. Am. Chem. Soc.* **2014**, *136*, 7662−7668.

(51) Kobayashi, S.; Higashimura, H. *Prog. Polym. Sci.* **2003**, *28*, 1015−1048.

(52) Lee, Y. E.; Cao, T.; Torruellas, C.; Kozlowski, M. C. *J. Am. Chem. Soc.* **2014**, *136*, 6782−6785.

(53) Li, Y.; Zhang, P.; Wu, M.; Liu, W.; Yi, Z.; Yang, M.; Zhang, J.; Zhang, G.; Bai, Z. *Chem. Eng. J.* **2009**, *146*, 270−274.

(54) Gao, Y.; Hu, G.; Zhong, J.; Shi, Z.; Zhu, Y.; Su, D. S.; Wang, J.; Bao, X.; Ma, D. *Angew. Chem., Int. Ed.* **2013**, *52*, 2109−2113.

(55) Zombeck, A.; Drago, R. S.; Corden, B. B.; Gaul, J. H. *J. Am. Chem. Soc.* **1981**, *103*, 7580−7585.

(56) Yang, J. H.; Sun, G.; Gao, Y.; Zhao, H.; Tang, P.; Tan, J.; Lu, A. H.; Ma, D. *Energy Environ. Sci.* **2013**, *6*, 793−798.

(57) Enoki, T.; Kobayashi, Y.; Fukui, K. I. *Int. Rev. Phys. Chem.* **2007**, *26*, 609−645.